AIAA Journal, Volume 56, Issue 12, 2018, pp. 4697-4705
DOI: 10.2514/1.J056293

Bio-inspired low-noise wing design for a two-winged flapping wing Micro Air Vehicle

Zhenbo Lu[1], Marco Debiasi[2], Quoc-Viet Nguyen[3] and Woei-Leong Chan[4]
[1,3,4]*Temasek Laboratories, National University of Singapore, 5A Engineering Drive 1, Singapore, 11741*
[2]*Centre for Defence Engineering, Cranfield University, Defence Academy of the United Kingdom Shrivenham, Swindon SN6 8LA, United Kingdom*

This work investigates the acoustic and thrust performance of different wing designs for a two-winged flapping-wing micro air vehicle (FW-MAV). The reference wings, made of a Mylar film membrane supported by carbon-fiber rods, produce a perceived overall noise of about 68.8 dBA when operating at the flapping frequency of 10 Hz typically required for flying such a flapping wing vehicle. This noise is much higher than the value of the environmental background. Wings of various materials and structural configurations have been designed and tested in order to reduce the flapping-wing noise. Sound and force measurements have been used to assess their acoustic and lift capabilities. It was found that a wing made with a highly elastic dielectric elastomer membrane can reduce the overall perceived noise of the flapping wing by 12 dBA while slightly increasing the thrust. The mechanisms leading to this noise reduction and their potential applications in quiet FW-MAVs are discussed.

Nomenclature

f_s = sampling rate

f_{LP} = frequency range for a low-pass filter

p' = fluctuating acoustic pressure

p_{ref} = reference acoustic pressure, $20\mu Pa$

SPL = sound pressure level

f = frequency

[1] Research Scientist, Temasek Laboratories, National University of Singapore, tslluz@nus.edu.sg.
[2] Research Fellow, Centre for Defence Engineering, Cranfield University, Marco.Debiasi@cranfield.ac.uk.
[3] Research Scientist, Temasek Laboratories, National University of Singapore, tslnqv@nus.edu.sg.
[4] Research Scientist, Temasek Laboratories, National University of Singapore, tslcwl@nus.edu.sg.

OASPL = overall sound pressure level

f_{upper} = highest frequency of interest

I. Introduction

RECENTLY, micro air vehicles (MAVs) have attracted an increasing research interest. MAVs have great potential to be used in both military and civil engineering applications such as sensing and information gathering. There are three main MAV concepts: fixed-wing MAV, rotary-wing MAV, and flapping-wing (FW) MAV [1–8]. Among these concepts, the insect-like flight characteristics of FW-MAVs are very desirable for flying indoor and in confined spaces. Many research groups have been working on developing FW-MAVs based on the principles of birds and insects flapping-type of flight. Three well-known FW-MAV prototypes are the DelFly from Delft University of Technology [9], the RoboBee from Harvard University [10], and more recently the FlowerFly from the National University of Singapore, Fig. 1.

Flapping flight is quite complex because of its highly-unsteady aerodynamics phenomena at low Reynolds numbers. Thus, the corresponding aerodynamic forces are very difficult to quantify mathematically since they cannot be straightforwardly calculated like for fixed wing. Several experimental [11-13] and numerical [14-16] research works have been done for investigating the unsteady aerodynamic forces of flapping wings of insect flight. Conversely, the sound generated by flying insects has received less attention even if the characteristics of this sound and the corresponding sound-generation mechanisms are particularly important both for the insect physiology's fundamental studies and their real bio-mimetic engineering applications. While the buzzing noise from bees or mosquitoes is sometimes used for mutual communication [17-18], it is primarily the by-product of their wings' flapping motion to produce thrust. More precisely, the sound is generated by the complex vortices and their interactions around the flapping wings that include three main vortices: leading edge vortex, trailing edge vortex and wing tip vortex [19-21]. The dominating sound sources are expected to be of a dipole type consisting of a) the wings motion, b) the vortex-structure interactions, and c) permeability [22].

Due to the weight limitation of FW-MAVs, passive noise control currently is the appropriate strategy for quieting their flapping wings. Looking at nature, insects, which have stiff and rigid wings made of chitin [23], are noisy flyers. The notable exceptions are butterflies and moths, the latter in particular having evolved soft, velvety wings with serration for silencing their noise. The architecture of these wings in some ways parallels that of owls whose extremely quiet flight capabilities have drawn great interest [24-25]. We did not attempt to replicate in detail

the features of these wings for application in FW-MAVs due to the micro-manufacturing challenges involved in their fabrication. We only approximately emulated their mechanical properties by using some types of fabric for the construction of wing membranes. At the same time, we drew inspiration from bats that have also evolved quiet flapping wings with a membrane structure resembling that of typical FW-MAVs, Fig. 1. Bats can move their fingers to adjust the stiffness or the tension of their wings' skin membranes [26-27] and use this to control their acoustic and aerodynamic performance in gusty or highly unsteady flow conditions.

Dielectric elastomer (DE) film is a modern, soft, smart actuator [28-29] which has fast response (<1 ms), high-efficiency (80%–90%) and can be used as a lightweight, high-energy-density, and high-strain (>200%) membrane. Its stiffness can be modulated by applying an external voltage and this tunable characteristic has been used for noise reduction applications [30-37]. Therefore, once the corresponding power supplies will be small and light enough, it has the potential to be used for creating an active bat-inspired membrane wing. In the meantime, this and other materials, can be tailored for creating FW-MAV wings with passively-reduced noise without sacrificing their aerodynamic characteristics. Along this line of thinking, the objective of this work is to investigate the noise and thrust generated by different wings installed on a two-winged FW-MAV model and to explore the preferable wing materials and configurations which can reduce the noise generated by this model, ideally to an average noise level similar to the inside of a household (about 50dBA). To this aim different membrane materials, including DE types, and different configurations of their supporting frames have been used for fabricating wings to be mounted on the flapping-wing model and their noise was measured in an anechoic chamber while the thrust was recorded by force transducers.

II. Materials and methods

A. The flapping-wing mechanism and wings

The flapping mechanism for a two-winged MAV, Fig. 2a), developed by Nguyen et al. [38] was used in the present study. As shown in Fig. 2b), gears and conventional four-bar (crank-rocker) linkages are combined together to create a flapping mechanism with one degree of freedom. The system is designed to convert the rotary motion of the motor into a flapping motion with stroke angle of 125º through a 2-stage gearbox of overall gear ratio 1:16 followed by an input link, output link and coupler with length of 4.5 mm, 5 mm and 12 mm respectively. A brushless motor (Hobby King AP-05) and an electronic speed controller are utilized for driving the flapping mechanism. A control box incorporating a tachometer, a pulse-width-modulation (PWM) generator and the power

supply (voltage: 4.2V, current: 5A) was designed and fabricated for controlling the brushless motor. The flapping frequency is measured by a Hall-effect sensor installed in the mechanism which sends the measured data to the control system for display or recording.

Various types of wings were fabricated and tested which are shown in Fig. 3. They are all referred to the same geometry shown in Fig 2c) and have wingspan (from wing tip to wing tip) of 240 mm once mounted in the flapping mechanism. The wings mainly differ from each other in their materials whose properties are shown in Tab. 1. These can be classified into three main types: the reference, insect-inspired wing (A), fabric-based wings inspired by owls/moths (B and C), and elastic wings inspired by bats (D, E, F, G, and H). Some wing types (G and H) were made in more than one configuration, which differ from each other by changes of the wing's root (slack) angle or by incorporating additional stiffening rods along the wing's trailing and tip edges. Such alterations of the structural configuration can change the flapping motion and the fluid-structure interactions around the wings due to different wing stiffness and wing inertia effects.

B. Experimental setups

An anechoic chamber whose inner dimensions are 2350mm×2350mm×2350mm was used for the present acoustic measurements, Fig. 4a). The inner walls of the chamber are covered by polyurethane-foam acoustic wedges (Illbruck SONEXsuper) whose absorption coefficient is larger than 1 at frequencies higher than 500 Hz. The two-winged FW-MAV model is placed at the center of the anechoic chamber, supported about 600 mm above the floor wedges by a firmly-fixed cantilevered beam that avoids vibrations generated by the flapping motion. With this setup, the flow generated by the FW-MAV propagates downward the anechoic chamber's ground, so it does not directly impinge on the microphone. The noise generated by the FW-MAV is recorded with a Brüel & Kjær Model 4953 1/2 inch condenser microphone with frequency response from 3 to 10,000 Hz (flat from 10 to 3000 Hz) connected to a microphone preamplifier (Brüel & Kjær Model 2669) and NEXUS 2690-A signal conditioner. The analog signal of the microphone is sampled at $f_s = 100$ kHz by a National Instruments NI-PCI-6014 analog-to-digital card which is installed in a computer. Each measurement consists of 10^6 samples. The microphone is installed on a support structure which can move it along a circle path around the FW-MAV with the help of a step servo motor, Fig. 4b). Since the wings and the experimental setup are symmetrically designed, the noise from 180º to 360º is the same as from 0º to 180º, so sound measurements were conducted only from 0º to 180º.

To avoid aliasing, a Butterworth filter was used to low-pass filter the signals at $f_{LP} = 0.499 f_s - 1$ (49,899 Hz). The corresponding power spectrograms were calculated using a short-time Fourier transform (4096 points) with Hann windows having 95% overlap. This provides a resolution of about 24 Hz. The power spectrograms of the voltage were converted to the power spectrograms of p'/p_{ref} using the sensitivity of the microphone (47.9 mV/Pa) and accounting for the amplifier's gain, where p' is the fluctuating acoustic pressure and $p_{ref} = 20\mu Pa$ is the reference acoustic pressure. The power spectrograms of p'/p_{ref} were converted into decibels and time averaged to give sound-pressure-level spectra $SPL(f)$ as a function of the acoustic frequency f. In order to calculate the relative loudness perceived by a human ear, the A-weighting correction is applied to the SPL spectra. The corresponding overall sound pressure level (OASPL) can be calculated by integrating the SPL spectra:

$$\mathrm{OASPL} = 10 log_{10} \int_0^{f_{\mathrm{upper}}} 10^{0.1 SPL(f)} df \quad (1)$$

where f_{upper} is the highest frequency of interest which is 10 kHz in this study.

The average thrust generated by the FW-MAV with different wing configurations was measured by installing it on a 280-mm high (5 times the wing's chord), slim, and stiff pillar with flared pedestal, Fig. 4c). This was placed on the top surface of a balance (AND EK-1200i) whose measuring range is from 0 g to 1200 g and resolution is 0.1 g. Installing the FW-MAV on such pillar reduced the effect of the flow generated by the FW-MAV on the balance and the platform' surfaces. In addition to the average thrust measurements, the time-dependent thrust generated by the flapping wings was measured with the setup shown in Fig. 4c) by using an ATI Nano17 SI-16-0.1 load cell whose force range and accuracy in the measured direction are 28.2 N and $\pm$ 5.2·10^{-3} N, respectively. The analog signal of the load cell was sampled at 5 kHz by a fast analog-to-digital board (National Instruments PCI 6221) installed in a computer similar to the one used for microphone acquisition. Each recording consists of 5×10^4 samples which were low-pass filtered at 40 Hz, i.e. 4 times the highest-flapping frequency used.

III. Results and discussions

Noise measurements of the different wing types were recorded at various flapping frequencies. Ideally all the wings should have reached a flapping frequency of 10 Hz to 12 Hz which is the typical value for flying the FlowerFly. But this flapping frequency could not be achieved by some wings due to their weight and attendant inertia. Depending on the wing type, a maximum flapping frequency of 8 or 10 Hz was achieved except the baseline

wing A. Also, it was found that the acoustic emission along the circle path is almost the same, thus the noise was measured at 90° and this angle is utilized as a reference for comparing the acoustic performance of various wings.

A. Acoustic characteristics of insect-inspired wings

Mylar film is a widely-used material for the fabrication of flapping wings due its light weight and good mechanical and chemical properties. This transparent and strong polymer in some ways resembles the chitin of many insects' wings and has been chosen as the wing membrane for the reference wing A to which the other wing types will be compared. Wing A has a 15μm thick Mylar film membrane and overall wing weight (inclusive of its supporting carbon-fiber rods) of 0.4g. It generates a high-level noise when flapping which is due to the wrinkling of its somewhat rigid membrane.

The SPL spectra of the flapping mechanism without wings and with wing A measured at 90º and at the flapping frequency of 8.0 Hz (the highest flapping frequency common to all the tested wings) is shown in Fig. 5a). There are three strong spectral peaks for the flapping mechanism with no wings, the lowest being at about 1100 Hz. This is close to the frequency of 1152 Hz calculated by multiplying 9 (the number of commutators inside the motor) by 128.0 Hz (the rotation speed of the motor which is equal to the gear ratio times the flapping frequency, i.e. 16 × 8 Hz). The other two peaks appear to be the second and third harmonics of the first one. With wing A, the amplitude of the 1100 Hz peak increases, possibly indicating that the flapping mechanisms generates more noise with the load from the wings. Conversely, the harmonics of the first peak are just recognizable as they are engulfed in the intense broadband noise generated by the flapping wings.

The OASPL values measured at flapping frequencies from 3.0 Hz to 10.0 Hz are plotted in Fig. 5b). In this and in the successive OASPL figures, the solid lines indicate the experimental results. The noise generated by the wings increases slightly less than linearly with the flapping frequency whereas that generated by the flapping mechanism alone increases linearly (albeit at a lower rate) up to 8.0 Hz above which it shows minimal increment. Based on the analysis of flexible pitching airfoils at high-Reynolds numbers, Manela also found that the generated sound increases with the flapping frequency albeit more than linearly, a discrepancy likely due to the different types of wing motion and of flow conditions considered.[39] The OASPL values of the mechanism alone and with wing A flapping at the frequency of 8.0 Hz are 50.3 dBA and 65.0 dBA, respectively. Based on the trend of its curve, the noise of the flapping mechanism alone at flapping frequencies of practical interest (> 10 Hz) should be marginally higher than 50.0 dBA, i.e. close to our target for a quiet FW-MAV. But the noise produced with wing A exceeds this

value by at least 18.5 dBA. Thus, suppressing the noise generated by the motor and the flapping mechanism is less significant than suppressing the noise produced by the flapping wings which therefore is the best option to quiet a FM-MAV.

B. Acoustic characteristics of owls/moths-inspired wings

In order to suppress the flapping noise generated by the wrinkling of the Mylar membrane of wing A, two fabric materials for making the membrane were tested. Both materials are more flexible than the Mylar film, thus, reducing wrinkling and its noise. At the same time their fibrous surfaces, while not as sophisticated as those of owls' feathers or moths' wings, could help in hushing the flapping noise. Wing B is fabricated with 7 Denier Nylon ultra-lightweight fabric (Formosa Taffeta Co. Ltd) which is a non-porous woven fabric and the lightest among all the wing membranes. Wing C is fabricated with non-woven fabric which has porosities passing through the material.

As shown in Fig. 6a), replacing Mylar with fabric can reduce the noise by more than 10 dBA at flapping frequencies of practical interest. The flapping-wing noise is about 5.0 dBA larger than the noise produced by the flapping mechanism alone and within 10 dBA from the 50 dBA target. Figure 6b) shows the corresponding average thrust measured in grams. Both fabric-based wings produce less thrust than the Mylar-based one with wing C suffering a larger performance penalty which we attribute to the leakage of air through its fabric porosities. Notably, the OASPL of the wings increases less than linearly with the flapping frequency whereas the thrust increases more than linearly, a result common to all the wings in this study. Thus, the corresponding values of OASPL per unit thrust (normalized OASPL) decrease with increasing the flapping frequency, Fig. 6c). This is a useful metric for evaluating the acoustic performance of flapping wings for lifting a MAV of prescribed weight. Since the normalized OASPL are remarkably high in the low flapping-frequency range, Fig. 6c) presents only the normalized OASPL for flapping frequencies higher than 6.0 Hz. Therefore, though wing B has slightly worse acoustic performance than wing C, it is preferable due to its lower noise per unit thrust.

C. Acoustic characteristics of bat-inspired wings

The wing membrane (patagium) of bats is made of elastic skin [29]. Five elastic materials were selected and used for the fabrication of wings' membranes. Wing D is made of thin (20 μm) low-density polyethylene (LDPE) film which, while flexible, cannot undergo large deformations under the expected aerodynamic loads. Wing E and wing F are fabricated using natural rubber sheets with thickness of 140 μm and 100 μm, respectively, which have hyper-

elastic properties similar to those of the patagium. During the flapping motion, these wings elastically deform under the aerodynamic forces which can also be used for tailoring or augmenting the thrust produced by a FW-MAV. The membranes of wing G and wing H are made of VHB 4914-015 (150 μm thick) and VHB F9460PC (50 μm thick) DE film manufactured by 3M. The latter is the thinnest commercially available DE film. The inner stress of the hyper-elastic material can be reduced when an external voltage is applied to it and thus it could be used for fabricating actively-controlled flapping-wing membranes if suitably small and light power units will become available in the future. Until then we can only study their passive properties. Due to the very low Young's modulus of the DE films, wing G and especially the thinner wing H would undergo excessively large deformations during the flapping motion thus reducing their aerodynamic effectiveness. To prevent this, a small-diameter cotton wire has been added to the trailing edge of the membrane of wing H to constrain its deformation along the wing span while maintaining the flexibility of the overall wing. This resembles the natural skin reinforcement visible at the trailing edge of the patagium.

The OASPL values of wing D, E, and F are compared to those of wing A in Fig. 7a). Since, the present flapping mechanism is not designed for driving heavy wings ($\geq$ 1g) without incurring damage, the heavier wings E and F could only be tested at flapping frequencies up to 8 Hz. The hyper-elastic wings E and F produce similar noise and have better acoustic performance than the elastic wing D. Figure 7b) shows that the elastic-membrane wings have marginally higher thrust than the reference Mylar type. The corresponding normalized OASPL values are shown in Fig. 7c) and suggest that the noise per unit thrust of wings E and F could be 3 dBA/g lower than wing A whereas wing D has a performance intermediate between these. However, in practical application one should also consider that, compared to wing D, wings E and F add about 1 g to the mass of a MAV. Thus, a larger thrust with attendant more noise would be required to lift a MAV with such wings which in turn could reduce their advantage.

Figure 8a) compares the OASPL values of wing A, G, and H. Wing G could only be tested at flapping frequencies up to 8 Hz due to its weight. Wing G and wing H have similar OASPL at the measured flapping frequencies and the noise level is about 13 dBA lower than wing A. Both wings have better acoustic performance than wing A while producing slightly higher thrust, Fig. 8b). The corresponding normalized OASPL values are shown in Fig. 8c) and suggest that, at practical flapping frequencies, wing H has the lowest noise per unit thrust of all the tested wings (about 3 dBA/g lower than wing A). This positive performance is due to both of its good acoustic characteristics and higher thrust. Figure 9 shows an excerpt of the time-resolved thrust measurements

obtained for wing A and wing H at the flapping frequency of 10 Hz. The time trace of the periodic thrust of wing H has clearly larger amplitude than wing A. It is not yet clear if this advantage is caused by the characteristics of the thinner DE elastomer, or by the use of the small-diameter cotton wire attached to its trailing edge, or both. Further specific investigation would be required to clarify this. Finally, since wing H weights 0.6 g, i.e. merely 0.2 g more than wing A, the thinner DE elastomer as implemented in wing H represents a promising material for reducing the noise generated by FW-MAVs.

The SPL spectra of the flapping mechanism with wings A and H at the flapping frequency of 10.0 Hz is shown in Fig. 10. The SPL spectrum of wing A is much higher than that of wing H at all frequencies, likely due to the wrinkling of wing A's somewhat rigid membrane, Fig. 10a). Figure 10b) shows that both flapping wings produce noise peaks at frequencies corresponding to harmonics of the flapping frequency and these are more noticeable below 1500Hz. Wing H with elastic membrane cannot avoid these harmonic peaks but they are much lower than those generated by the wing A.

D. Additional configurations for wing H

The results obtained in the previous section prompted us to explore if some modifications of wing H could be introduced to simplify its configuration without sacrificing its positive qualities, and maybe improving them. The first modification, implemented in wing H1, is the elimination of the 10º slack angle at the wing root in favour of a simpler 90˚ connection between the rods supporting the leading and the root edges. The rationale for this is that the very elastic behavior of the thin DE elastomer should allow sufficient deformation of the wing membrane under the aerodynamic loads without requiring the extra amount of pliable surface introduced by the slack angle. Wing H2 has the same simplified geometry of wing H1 but replaces the small-diameter cotton wire at the trailing edge with a highly flexible 0.3 mm diameter carbon-fiber rod which is also added to its tip edge. The replacement of a wire (which can only resist to tension) with a thin flexible rod (which can additionally support some compression and flexion loads) would open up the possibility of fine tuning the mechanical properties of a wing membrane. Due to its slightly smaller membrane, wing H1 has marginally lower weight than wing H. However, the introduction of the additionally flexible rods in wing H2 increases its weight by about 10%.

The OASPL values of wings H, H1 and H2, Fig. 11a), appear to be very similar to each other. The same could be said of their thrust at the measured flapping frequencies. Wing H2 might have a slightly larger thrust at higher flapping frequencies, but this would require additional measurements to be confirmed. Consequently, the normalized

thrust of wings H1 and H2 is close to that of wing H with H2 possibly having a slightly better performance at flapping frequencies of practical interest (Fig. 11b) and 11c)). These results suggest that the above modification of wing H do not introduce any meaningful performance penalty while allowing some options in the manufacturing of the wings which can be used to further improve their performance.

In conclusion, as shown in Fig,5a) and Fig. 10a,b), the flapping wing noise consists of a series of harmonic peaks generated by the flapping motion of the wings and of broadband high-level SPL spectra likely generated by the wrinkling of the wing membranes. By keeping the same geometry of the wings, the harmonic peaks cannot be avoided using different types of membrane material, whereas the broadband noise can be significantly reduced using the hyper-elastic materials or feather-like soft fabric materials. Higher elastic material leads to larger noise reduction. The thrust is affected by the material used in as much it produces different deformation of the wings during the flapping and by the flow leakage through the membrane if this has some porosity as in the case of some fabric.

IV. Conclusion

Experimental measurements were performed of the noise and of the thrust of flapping wings for a micro air vehicle with the goal of identifying the configurations which produce the least noise per unit thrust. All the wings were mounted on a common flapping mechanism whose low overall perceived noise is close to the target set for this study. Most wings have the same basic geometry whereas different materials were used for fabricating their membranes. The reference-wing membrane is made of Mylar film, a common material used for such application, and produces a perceived overall noise of about 68.8 dBA when operating at a flapping frequency close to that typically required for flying a flapping-wing MAV. It was found that the overall noise of this and of the other wings increases less than linearly with increasing the flapping frequency whereas the thrust increases more than linearly. Thus, the noise per unit thrust, a useful metric for evaluating the acoustic performance of wings for lifting a MAV of prescribed weight, decreases with increasing the flapping frequency. This suggests that, all the other things being the same, flapping the wings at high rather than at low rate could be an effective method for quieting the flight of a flapping-wing MAV. At the same time, weight reduction is confirmed to be the preferred approach to increase the performance of a flying vehicle also in terms of noise reduction. Replacing Mylar film with two types of fabric shows good noise reduction but at the cost of reduced thrust. The use of hyper-elastic materials (natural rubber and

dielectric-elastomer sheets) resembling a bat's patagium also produces significant noise reduction without suffering thrust losses. A disadvantage of natural rubber membranes is their relatively high mass (at least with the thickness used in this study) which increases both the weight of the vehicle and the inertia of the wings which in turns prevents high flapping rates. The wing made with a thin dielectric elastomer has marginally higher weight than the Mylar one, is 13 dBA quieter, and produces 3 dBA/g lower noise per unit thrust, the lowest of all the tested wings. Modifications of the geometry and structure of this wing for improving its performance do not seem to adversely affect its acoustic advantage. In addition, the future development of suitably small and light power units could enable the active control of flapping-wing membranes made with dielectric elastomer.

References

[1] W. Shyy, M. Berg and D. Ljungqvist D, Flapping and flexible wings for biological and micro air vehicles, Progress in Aerospace Sciences, 35 (1999) 455–505.

[2] W. Shyy, Y. Lian, J. Tang, D. Viieru and H. Liu, Aerodynamics of low Reynolds number flyers, Cambridge University Press, New York (2008).

[3] T. J. Muller, Fixed and flapping wing aerodynamics for micro air vehicle applications, AIAA Progress in astronautics and aeronautics, 195 (2001).

[4] W. Shyy, P. Ifju and D. Viieru, Membrane wing-based micro air vehicles, Applied Mechanics Reviews, 58 (2005) 283–301.

[5] J. Pines and F. Bohorquez, Challenges facing future micro-air-vehicle development, Journal of Aircraft, 43 (2006) 290–305.

[6] Y. Lian, W. Shyy, D. Viieru and B. Zhang, Membrane wing aerodynamics for micro air vehicles, Progress in Aerospace Sciences, 39 (2003) 425–465.

[7] M. Platzer, K. Jones, J. Young and J. Lai, Flapping wing aerodynamics: progress and challenges. AIAA Journal, 46 (2008) 2136–2149.

[8] B. K. Stanford, P. Ifju, R. Albertani and W. Shyy, Fixed membrane wings for micro air vehicles: experimental characterization, numerical modelling and tailoring, Progress in Aerospace Sciences, 44 (2008) 258–294.

[9] C. H. E. de Croon, K. M. E. de Clercq, R. Ruijsink, B. Remes, C. de Wagter, Design, aerodynamics, and vision-based control of the DelFly, The International Journal on Micro Air Vehicles, 1 (2009) 71- 97.

[10] B. Finio, B. Eum, C. Oland and R. J. Wood, Asymmetric flapping for a robotic fly using a hybrid power-control actuator, IEEE/RSJ IROS, St. Louis, MO, USA (2009).

[11] C. P. Ellington, C. Van den Berg, A. P. Willmott and A. L. R. Thomas, Leading-edge vortices in insect flight, Nature, 384 (1996) 626–630.

[12] J. M. Birch and M. H. Dickinson, Spanwise flow and the attachment of the leading-edge vortex on insect wings, Nature, 412 (2001) 729–733.

[13] M. H. Dickinson, F. O. Lehmann and S. P. Sane, Wing rotation and the aerodynamic basis of insect flight, Science, 284 (1999) 1954–1961.

[14] Z. J. Wang, Two dimensional mechanism for insect hovering, Physical Review Letters, 85 (2000) 2216–2219.

[15] M. Sun and J. Tang, Unsteady aerodynamic force generation by a model fruit fly wing in flapping motion, Journal of Experimental Biology, 205 (2002) 55–70.

[16] M. Sun and J. Tang, Lift and power requirements of hovering flight in drosophila, Journal of Experimental Biology, 205 (2002) 2413–2427.

[17] S. Drosopoulos and M. F. Claridge, Insect sound and communication, Physiology, Behavior, Ecology, and Evolution, CRC press, Taylor and Francis Group, Florida, USA (2006).

[18] J. Sueur, E. J. Tuck and D. Robert, Sound radiation around a flying fly, The Journal of the Acoustical Society of America, 118 (2005) 530-538.

[19] C. Van den Berg and C. P. Ellington, The vortex wake of 'hovering' model hawkmoth, Philosophical transactions of the royal society of London series b-biological sciences, B352 (1997) 317-328.

[20] S. P. Sane, The aerodynamics of insect flight, Journal of Experimental Biology, 206 (2003) 4191-4208.

[21] M. S. Howe, Theory of Vortex Sound, Cambridge University Press (2002).

[22] M. Weidenfeld and A. Manela, On the attenuating effect of permeability on the low frequency sound of an airfoil, Journal of Sound and Vibration 375(2016), 275–288.

[23] R. F. Chapman, The Insects: Structure and function, 4th ed, Cambridge University Press, New York (1998).

[24] R. R. Graham, The silent flight of owls, The Aeronautical Journal, 38 (1934) 837-843.

[25] M. Lilley, A study of the silent flight of the owl, AIAA Paper No. 98-2340, 1998.

[26] S. M. Swartz, M. S. Groves, H. D. Kim and W. R. Walsh, Mechanical properties of bat wing membrane skin, Journal of Zoology, 239 (1996) 357–378.

[27] S. M. Swartz, K. L. Bishop and M. F. Ismael-Aguirre, Dynamic complexity of wing form in bats: implications for flight performance. Functional and evolutionary ecology of bats, edited by Z. Akbar, G. McCracken, and T. H. Kunz, Oxford University Press, Oxford, 2005, 110–130.

[28] R. Pelrine, R. Kornbluh, Q. B. Pei and J. Joseph, High-speed electrically actuated elastomers with strain greater than 100%, Science, 287 (2000) 836-839.

[29] A. O'Halloran, F. O'Malley and P. McHugh, A review on dielectric elastomer actuators, technology, applications, and challenges, Journal of Applied Physics, 104 (2008) No. 071101.

[30] Z. Lu, Y. Cui, J. Zhu, Z. Zhao and M. Debiasi, Acoustic characteristics of a dielectric elastomer absorber, The Journal of the Acoustical Society of America, 134 (2013) No. 4218.

[31] Z. Lu, Y. Cui, M. Debiasi and Z. Zhao, A Tunable Dielectric Elastomer Acoustic Absorber, Acta Acustica United with Acustica, 101 (2015) 863-866.

[32] Z. Lu, Y. Cui, J. Zhu and M. Debiasi, A novel duct silencer using dielectric elastomer absorbers, SPIE Smart Structures/NDE, San Diego, California, USA, 2014.

[33] Z. Lu, H. Godaba, Y. Cui, C. C. Foo, M. Debiasi and J. Zhu J, An electronically tunable duct silencer using dielectric elastomer actuators, The Journal of the Acoustical Society of America, 138 (2015) EL236.

[34] Z. Lu, Y. Cui and M. Debiasi, Active membrane-based silencer and its acoustic characteristics, Applied Acoustics, 111 (2016) 39–48

[35] X. Yu, Z. Lu, F. Cui, L. Cheng and Y. Cui, Tunable acoustic metamaterial with an array of resonators actuated by dielectric elastomer, Extreme Mechanics Letters 12 (2017) 37-40.

[36] X. Yu, Z. Lu, L. Cheng and F. Cui, Vibroacoustic modeling of an acoustic resonator tuned by dielectric elastomer membrane with voltage control, Journal of Sound and Vibration, 387 (2017) 114–126.

[37] Zhenbo Lu, Milan Shrestha, Gih-Keong Lau. Electrically tunable and broader-band sound absorption by using micro-perforated dielectric elastomer actuator. Applied Physics Letters 110(18), 182901 (2017).

[38] Q. V. Nguyen, W. L. Chan and M. Debiasi, Hybrid design and performance tests of a hovering insect-inspired flapping-wing micro aerial vehicle. Journal of Bionic Engineering 13(2) (2016) 235-248.

[39] A. Manela, On the acoustic radiation of a pitching airfoil, Physics of Fluids, 25 (2013), 071906.

Table 1: Properties of materials used for the wing membranes

Type	Material	Weight (g)*	Membrane thickness (μm)	Young's modulus (MPa)
Wing A	Mylar	0.4	15	602 - 1400
Wing B	7 Denier Nylon non-porous woven fabric	0.2	40	N. A
Wing C	porous non-woven fabric	0.6	270	N. A
Wing D	Low-density polyethylene (LDPE)	0.5	20	400
Wing E	Natural rubber (Oppo band)	1.1	140	5
Wing F	Natural rubber (Latex glove)	1.0	100	5
Wing G	3M VHB 4914-015 tape	1.3	150	0.22
Wing H	3M VHB F9460PC	0.6	50	0.22

* The weight includes the weight of wing structure and membrane.

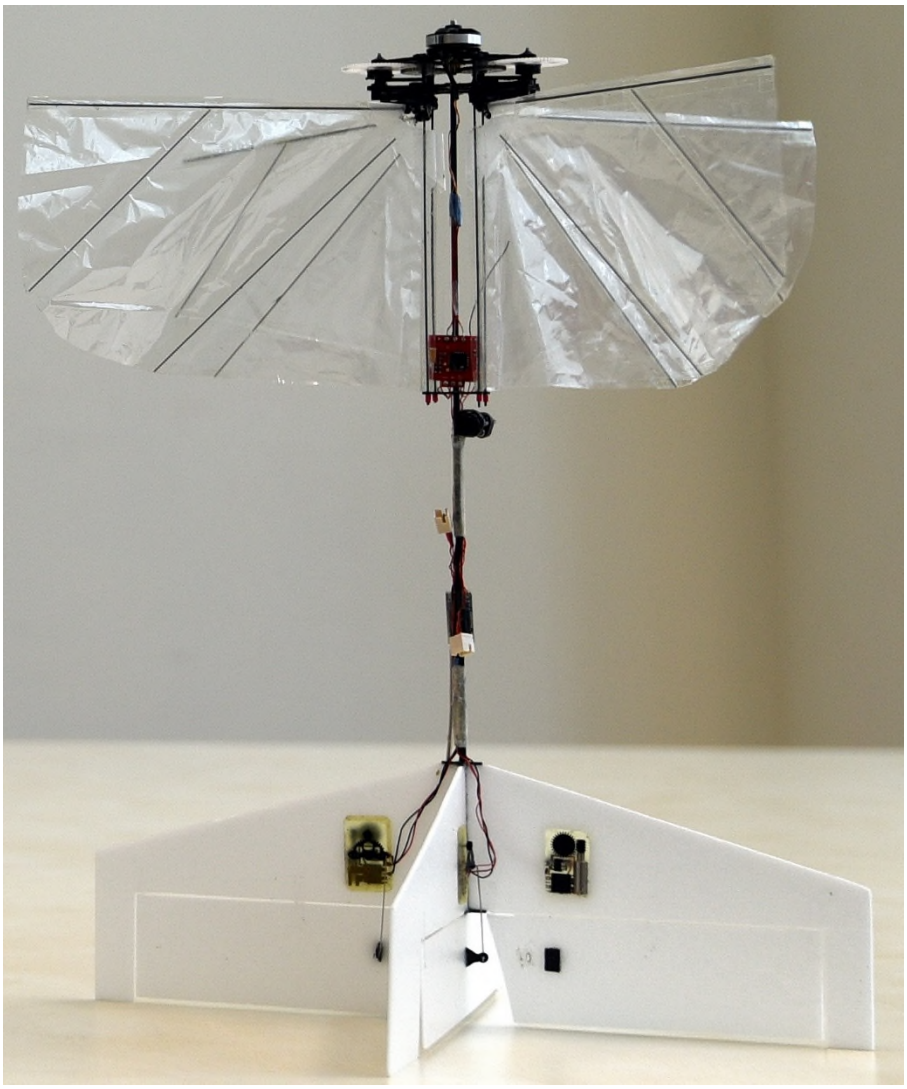

Figure 1: FlowerFly developed by the Temasek Laboratories of the National University of Singapore.

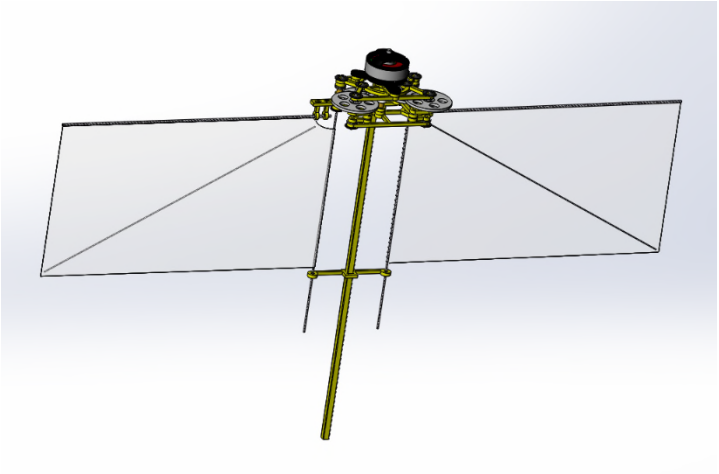

a)

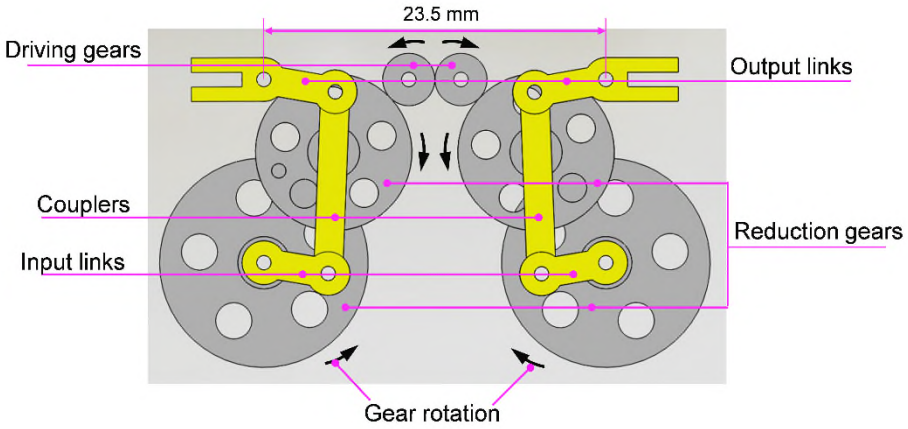

b)

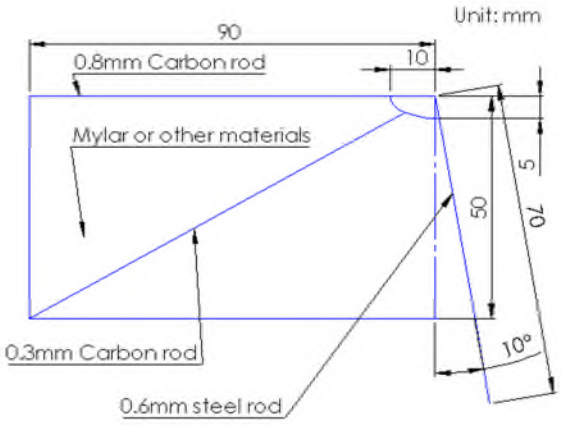

c)

Figure 2: flapping-wing model design: a) assembly of the flapping-wing model; b) crank-rocker mechanism using 4-bar linkage; c) reference wing geometry.

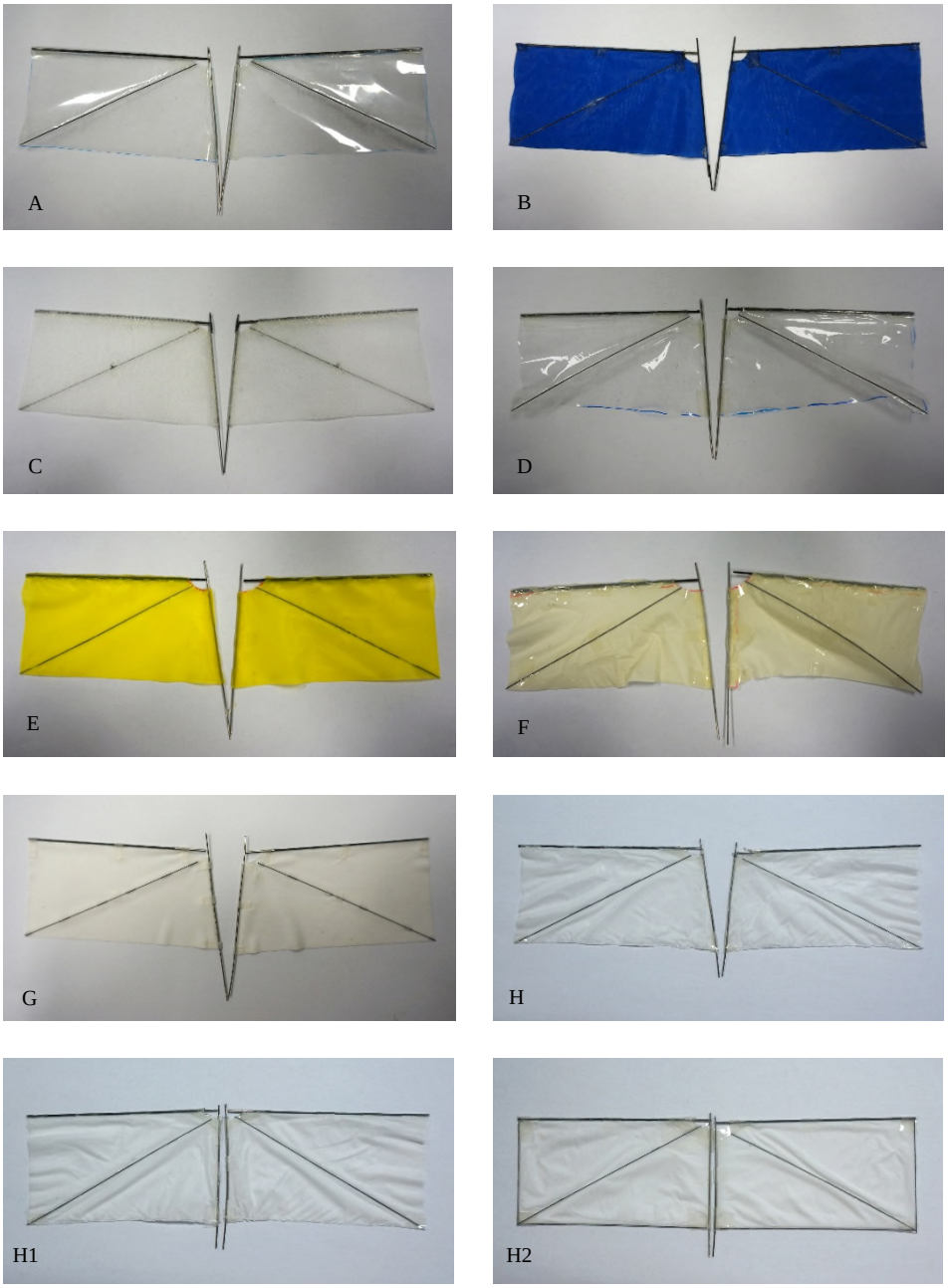

Figure 3: Different wing used in the experimental measurements.

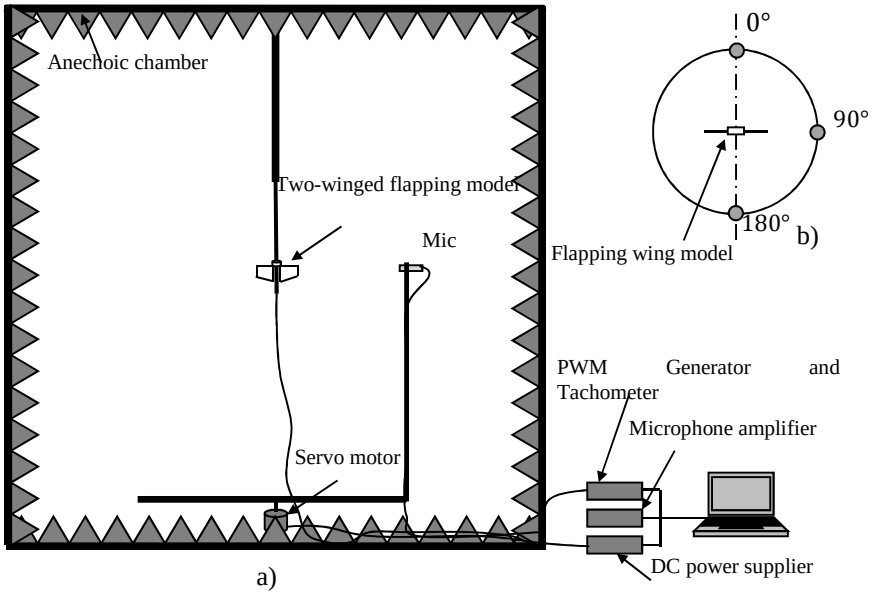

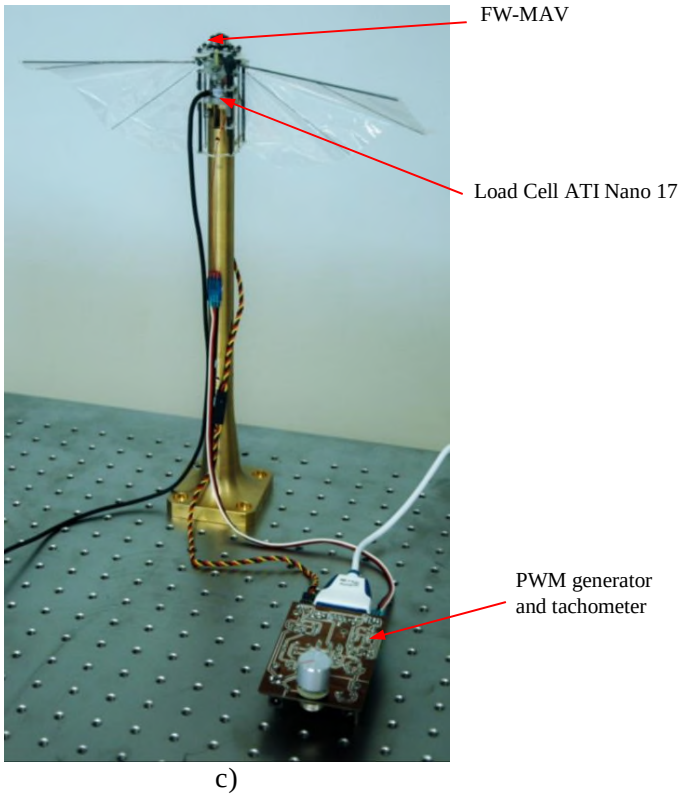

Figure 4: Experimental setup: a) side view and b) top view of the placement of the flapping-wing model and microphones inside the anechoic chamber; c) time-dependent thrust measurement system.

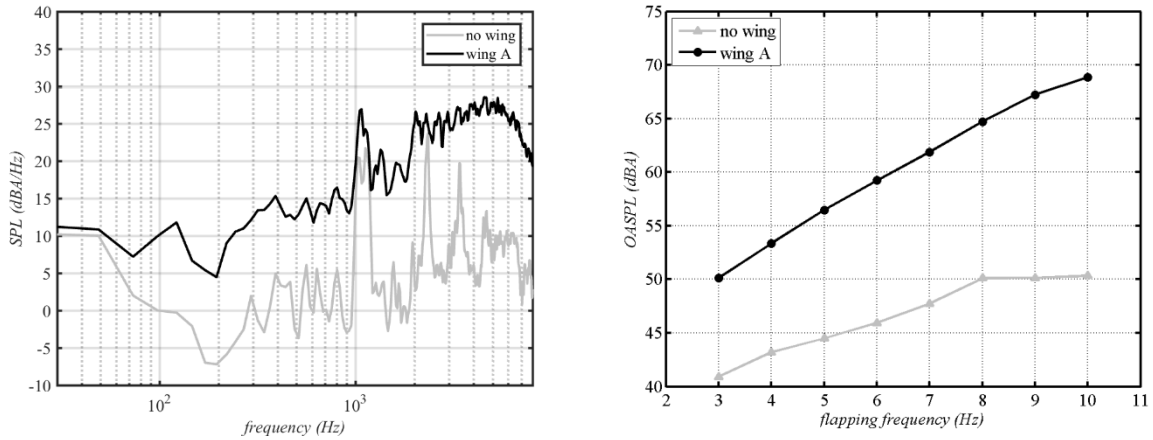

a) b)

Figure 5: Noise of the flapping mechanism alone (no wing) and with wing A: a) A-weighted SPL spectra at the flapping frequency of 8.0 Hz; b) OASPL values at various flapping frequencies. The noise was measured at 90°.

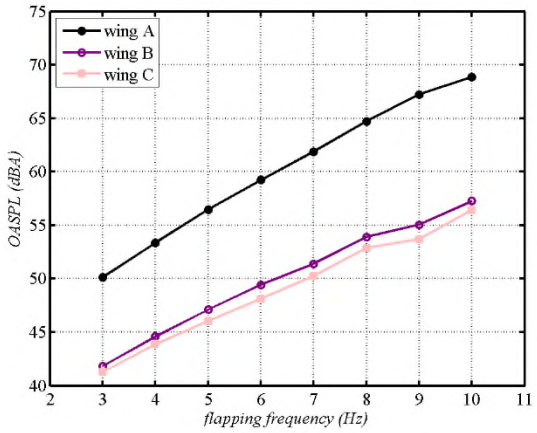

a)

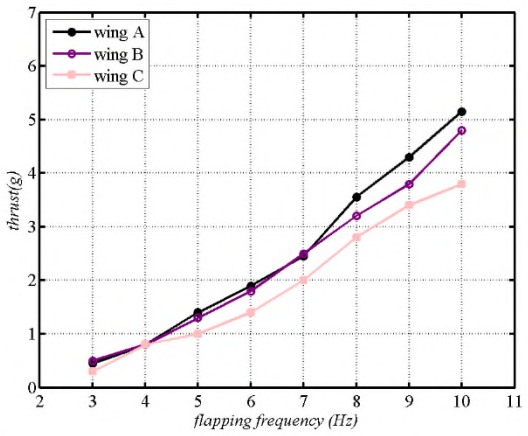

b)

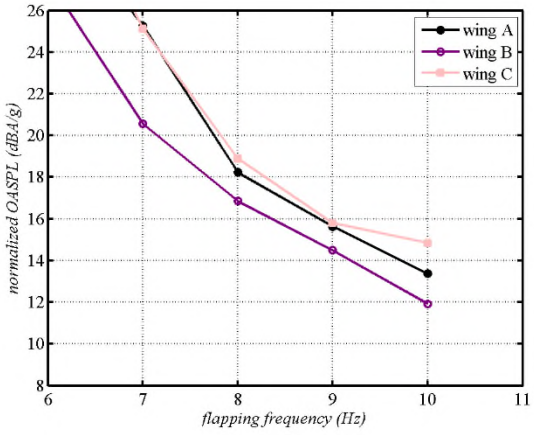

c)

Figure 6: Performance of wings A, B, and C at various flapping frequencies: a) OASPL; b) thrust; c) OASPL per unit thrust. The noise was measured at 90°.

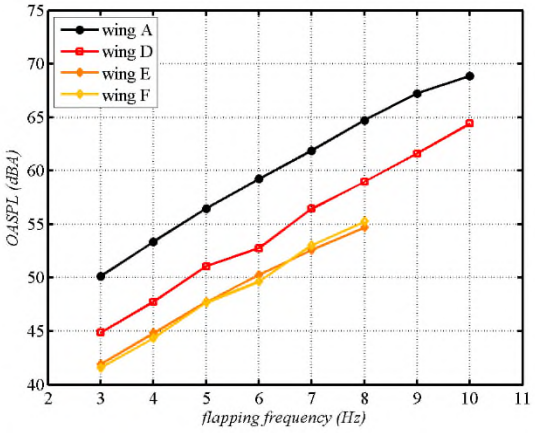

a)

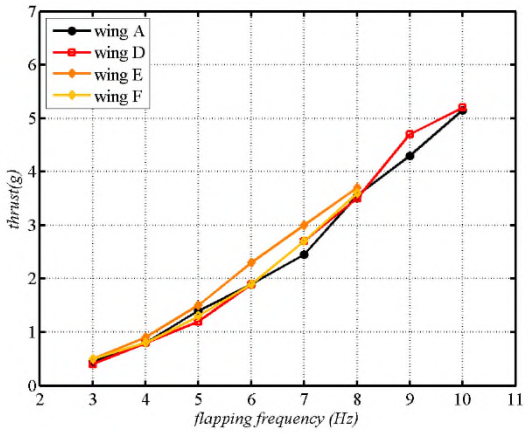

b)

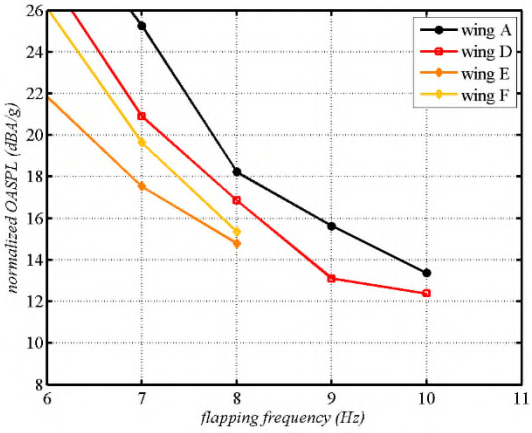

c)

Figure 7: Performance of wings A, D, E, and F at various flapping frequencies: a) OASPL; b) thrust; c) OASPL per unit thrust. The noise was measured at 90°.

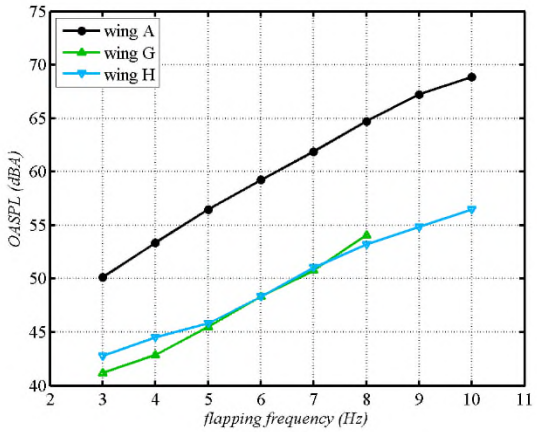

a)

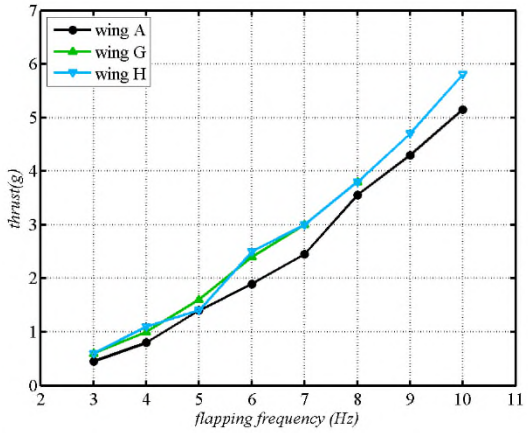

b)

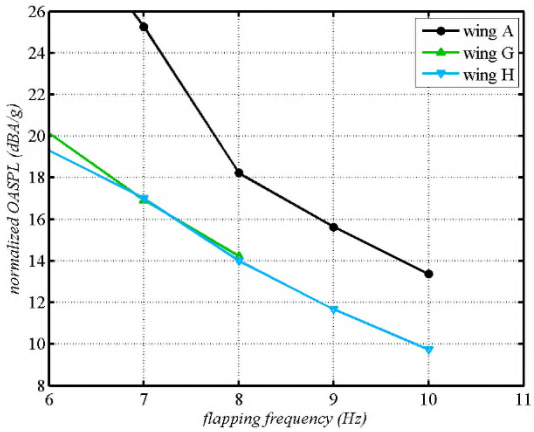

c)

Figure 8: Performance of wings A, G, and H at various flapping frequencies: a) OASPL; b) thrust; c) OASPL per unit thrust. The noise was measured at 90°.

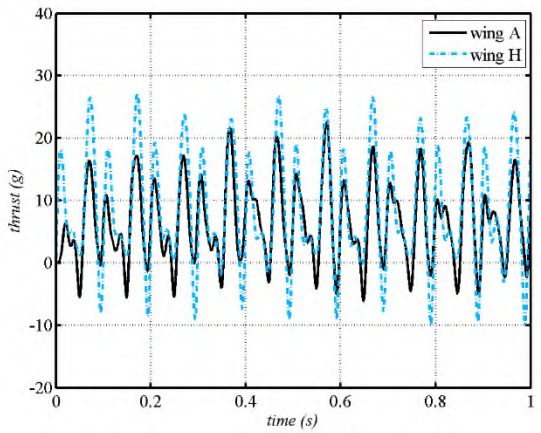

Figure 9: Time-resolved thrust of wing A and wing H flapping at 10 Hz.

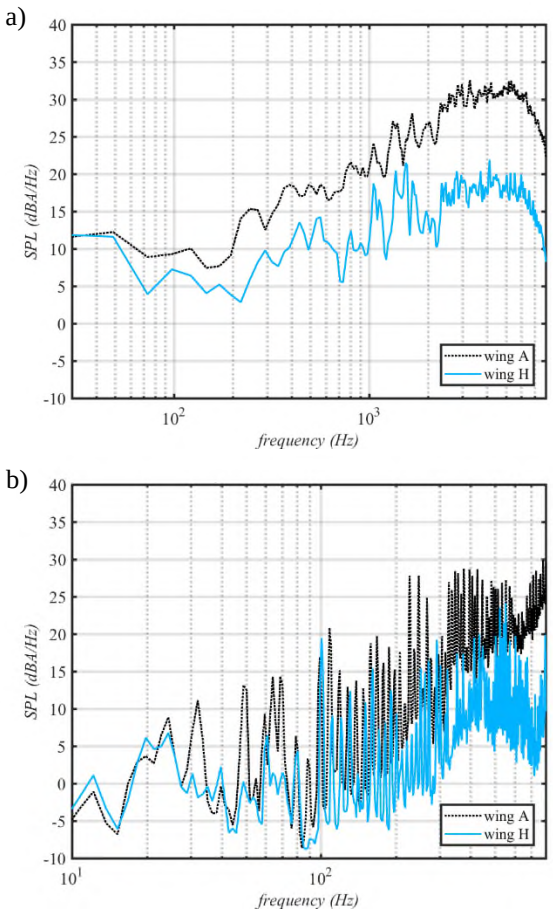

Figure 10: Noise of the flapping mechanism with different wings at the flapping frequency of 10.0 Hz: a) A-weighted SPL spectra, frequency range from 5 Hz to 8 kHz; b) A-weighted SPL spectra, frequency range from 5 Hz to 800 Hz using a short-time Fourier transform (65536 points) with Hann windows having 95% overlap. The noise was measured at 90°.

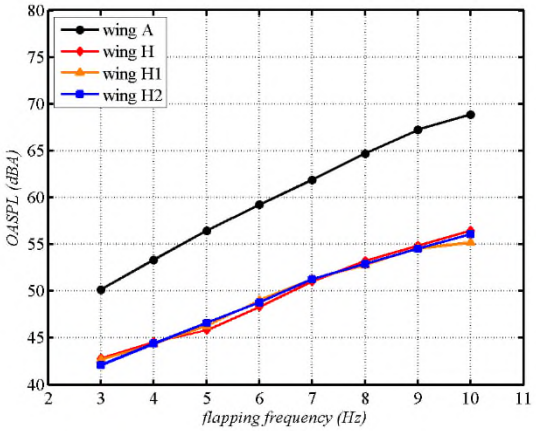

a)

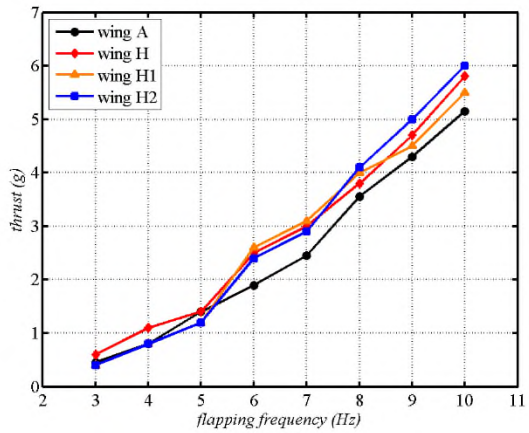

b)

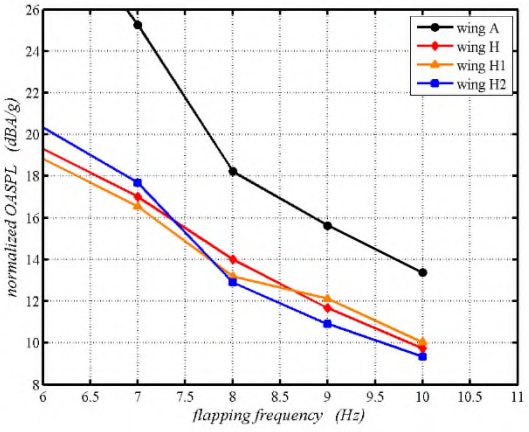

c)

Figure 11: Performance of wings A, H, H1, and H2 at various flapping frequencies: a) OASPL; b) thrust; c) OASPL per unit thrust. The noise was measured at 90°.